

# Dynamics of a Circular Cylinder and Two Point Vortices in a Perfect Fluid

Sergey M. Ramodanov<sup>1\*</sup> and Sergey V. Sokolov<sup>2\*\*</sup>

<sup>1</sup>*Financial University under the Government of the Russian Federation,  
Department of Data Analysis and Machine Learning,  
4th Veshnyakowski pr. 4, 125993 Moscow, Russia*

<sup>2</sup>*Moscow Institute of Physics and Technology (State University),  
Institutskiy per. 9, Dolgoprudny, 141701 Moscow, Russia*

Received August 05, 2021; revised October 29, 2021; accepted November 03, 2021

**Abstract**—We study a mechanical system that consists of a 2D rigid body interacting dynamically with two point vortices in an unbounded volume of an incompressible, otherwise vortex-free, perfect fluid. The system has four degrees of freedom. The governing equations can be written in Hamiltonian form, are invariant under the action of the group  $E(2)$  and thus, in addition to the Hamiltonian function, admit three integrals of motion. Under certain restrictions imposed on the system's parameters these integrals are in involution, thus rendering the system integrable (its order can be reduced by three degrees of freedom) and allowing for an analytical analysis of the dynamics.

MSC2010 numbers: 76M23, 34A05

DOI: 10.1134/S156035472106006X

Keywords: point vortices, Hamiltonian systems, reduction

## 1. INTRODUCTION AND HISTORICAL COMMENTS

The dynamics of vortices-body systems has been extensively studied in the classical hydrodynamics (e. g. Karman's wake, Joukowski hydrofoil). The fact is that real fluids are viscous and a body immersed in such a fluid experiences not only superficial friction but is also subject to forces due to the vorticity produced by the body itself (e. g., the vortices peeled off from the body's sharp edges). Obviously, such real-life mechanical systems can hardly be explored analytically as this implies the analysis of Navier–Stokes equations with boundary conditions on moving surfaces.

At the same time, the 2D ideal-liquid model (in spite of its simplicity) offers the advantage of using governing ODEs for interacting vortices-body systems. Of course, in the case of an ideal fluid an originally vortex-free flow cannot gain any vorticity. So one has either to postulate vortex shedding from a body [25, 39] or assume that the flow was vortical from the very beginning. Until quite recently the interaction of the body and surrounding flow was considered in a simplified setting: the body was assumed to be fixed (see, for example, the survey paper [19]) or to be moving in a prescribed manner. For example, the interaction between a rectilinearly moving cylinder and a single point vortex was studied in [16]. Dynamics of two vortices inside a circular domain filled by a perfect fluid or a Bose–Einstein condensate can be found in [29, 37, 38].

Let us give a brief outline of the rigorous *analytic* results (which are really few) concerned with the *dynamical* interaction between bodies and vortical flows. One of the simplest manifestations of vorticity is a nonzero circulation of the flow's velocity around the body. The motion of a smooth body (e. g., a wing) in the presence of gravity was considered by Chaplygin [12]; the circulation around the body was assumed constant. Later this problem was studied in, for example, [22, 27], a detailed analysis can be found in [7]. In particular, due to the circulation the body remains within

\*E-mail: ramodanov@mail.ru

\*\*E-mail: sokolovsv72@mail.ru

a certain horizontal strip in the course of motion [27]. Further generalizations and extensions of the problem (including introduction of external periodic forces or assuming the circulation to be a periodic function of time) are considered in [9, 11, 17].

The problem of dynamical interaction of a 2D rigid body (also referred to as *cylinder*) with point vortices in a perfect fluid can be seen as another important step in understanding (*analytically*, not numerically) the effect of vorticity on an immersed body. The Hamiltonian approach to the analysis of the dynamics of point vortices, which traces back to Kirchhoff [21], was further developed [6, 8, 26, 32] and adapted to the case where point vortices interact dynamically with a cylindrical rigid body. In [26] and then in [32] *exact* equations of motion were obtained; moreover, in [26] formulas for the hydrodynamics force and moment imposed on a body of arbitrary (not necessarily circular) shape are derived. Integrability of the system that consists of a circular cylinder and a single point vortex was proved in [6], bifurcations of Liouville tori was discussed in [10]. In [8], some partial solutions were found for this system and the qualitative picture of motion was studied in greater detail. The dynamics of a *heavy* circular cylinder interacting with a point vortex is explored in [36], and in a case of  $N$  vortices in [35].

So a system that consists of a circular cylinder and only one point vortex is integrable; if there are two or more vortices the system becomes nonintegrable [8, 33, 34]. However, if there are *exactly two* vortices, then under certain additional restrictions: 1) the total linear momentum of the system is zero and 2) the total circulation of the fluid (i.e., circulation along the contour that encloses the entire system) is zero, the system remains integrable [8, 24]. Note that the strengths of the two vortices  $\Gamma_1$  and  $\Gamma_2$  are arbitrary (they do not necessarily form a vortex pair with  $\Gamma_1 = -\Gamma_2$ ). So this paper deals with this special case.

It should be noted that the system that consists of a cylinder and *two* vortices has been considered in a number of works. The paper [31] proves the existence and studies the stability of a special solution when a circular cylinder and a vortex pair (two vortices with intensities equal in magnitude and opposite in sign) are moving along parallel straight lines. This solution can be justly considered a dynamical counterpart of the famous Föppl equilibrium of a vortex pair in a uniform flow past a fixed circular cylinder. Analogous results for the case of an elliptic cylinder were obtained in [18]. The motion of two point vortices and a circular foil in the presence of periodic excitation caused by a material massive point moving inside a foil is studied in [2]. In [15] the interaction of a circular cylinder with a vortex pair is studied numerically. Mention should also be made of the recent work [4] investigating the stability of two equal vortices and a circular cylinder placed exactly in the middle between them.

## 2. EQUATIONS OF MOTION AND CONSERVED QUANTITIES

### 2.1. Formulation of the Problem and the Governing Equations

Consider a 2D rigid body of circular shape (a circular cylinder) moving in an unbounded volume of perfect fluid which is at rest at infinity. In the fluid outside the body there are two point vortices with strength  $\Gamma_1$  and  $\Gamma_2$ . The flow is assumed to be incompressible and otherwise irrotational. In the general case, the circulation of the flow about the cylinder is  $\Gamma$  (Fig. 1). (More exactly,  $\Gamma$  is the circulation of the fluid's velocity along a contour that encloses both the body and the vortices; equally  $\Gamma$  can be considered the flow's circulation along the cylinder's boundary when the vortices vanish, that is,  $\Gamma_1 = \Gamma_2 = 0$ .) The objective of the paper is to reduce explicitly the governing equations to a one-degree-of-freedom Hamiltonian system which, in its turn, allows for a detailed examination of the system's dynamics.

There is a reason why there are exactly two vortices (the governing equations could be easily written out for an arbitrary number of vortices). As mentioned above, the system of a circular cylinder and two point vortices is integrable provided the impulse of the system and the circulation about the cylinder are zero.

Let us introduce the following notation (Fig. 1):  $\mathbf{r}_c = (x_c, y_c)$  is the radius-vector from the origin of a fixed coordinate system  $Oxy$  to the cylinder's center,  $\mathbf{v} = (v_1, v_2)$  is the velocity of the cylinder,  $\mathbf{r}_j = (x_j, y_j)$  is the vector from the center of the cylinder to the  $j$ th vortex,  $R$  stands for the cylinder's radius,  $a$  is the effective mass (mass+added mass) of the cylinder, the constants  $\lambda$

and  $\lambda_1, \lambda_2$  are related to the circulation about the cylinder and the strengths of the vortices as  $\lambda = \frac{\Gamma}{2\pi}, \lambda_j = \frac{\Gamma_j}{2\pi}$ . To get rid of  $2\pi$  in the denominators, the fluid's density is chosen to be  $\frac{1}{2\pi}$ .

The complex potential of the flow along with the formulas for the hydrodynamic forces applied to the cylinder (necessary for obtaining the equations of motion) are presented in Appendix A. Omitting the derivation, we present the governing equations in the form [26, 28]:

$$\begin{aligned} \dot{\mathbf{r}}_j &= -\mathbf{v} + \text{grad}\varphi_j(\mathbf{r})|_{\mathbf{r}=\mathbf{r}_j}, \quad j = 1, 2 \\ \dot{\mathbf{r}}_c &= \mathbf{v}, \\ a\dot{v}_1 &= -\lambda v_2 + \lambda_1(\tilde{y}_1 - \dot{y}_1) + \lambda_2(\tilde{y}_2 - \dot{y}_2), \\ a\dot{v}_2 &= \lambda v_1 - \lambda_1(\tilde{x}_1 - \dot{x}_1) - \lambda_2(\tilde{x}_2 - \dot{x}_2). \end{aligned} \tag{2.1}$$

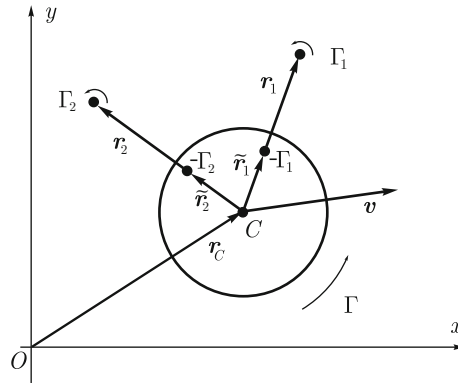


Fig. 1. A circular cylinder and two point vortices.

2.2. Conserved Quantities

The system of equations (2.1) has a first integral, which can be treated as an integral of energy [6]:

$$H = \frac{1}{2a}\mathbf{v}^2 + \frac{1}{2} \sum_{j=1}^2 \lambda_j^2 \ln(r_j^2 - R^2) - \frac{\lambda}{2} \sum_{j=1}^2 \lambda_j \ln(r_j^2) + \frac{1}{2} \lambda_1 \lambda_2 \ln \frac{R^4 - 2R^2(\mathbf{r}_1, \mathbf{r}_2) + \mathbf{r}_1^2 \mathbf{r}_2^2}{|\mathbf{r}_1 - \mathbf{r}_2|^2}. \tag{2.2}$$

In [6] it is shown that Eqs. (2.1) are Hamiltonian and this fact does not seem to stem from any Lagrangian origin. In that paper the following proposition is proved.

The governing equations (2.1) can be written in the following form:

$$\dot{\zeta}_i = \{\zeta_i, H\} = \sum_k \{\zeta_i, \zeta_k\} \frac{\partial H}{\partial \zeta_k}.$$

Here  $\zeta_i$  is the phase vector of this system, that is,  $\zeta = (x_c, y_c, v_1, v_2, x_1, y_1, x_2, y_2)$ , and  $H$  is the Hamiltonian function (2.2). The nonzero components of the tensor read

$$\begin{aligned} \{v_1, x_i\} &= \frac{1}{a} \frac{r_i^4 - R^2(x_i^2 - y_i^2)}{r_i^4}, & \{v_1, y_i\} &= -\frac{1}{a} \frac{2R^2 x_i y_i}{r_i^4}, \\ \{v_2, x_i\} &= -\frac{1}{a} \frac{2R^2 x_i y_i}{r_i^4}, & \{v_2, y_i\} &= \frac{1}{a} \frac{r_i^4 + R^2(x_i^2 - y_i^2)}{r_i^4}, \\ \{v_1, v_2\} &= \frac{\lambda}{a^2} - \sum_i \frac{\lambda_i}{a^2} \frac{r_i^4 - R^4}{r_i^4}, & \{x_i, y_i\} &= -\frac{1}{\lambda_i}, \\ \{x_c, v_1\} &= \{y_c, v_2\} = a^{-1}. \end{aligned} \tag{2.3}$$

Thus, Eqs. (2.1), which govern the system of a circular cylinder and two vortices, are a Hamiltonian system with four degrees of freedom. For the system to be integrable, three more integrals of motion (in addition to the Hamiltonian) are required; moreover, these integrals must be in involution with each other.

**Remark.** A more appropriate choice of basis functions [30] can provide a more elegant form of the bracket (2.3). However, from the methodological point of view, not the form of Eqs. (2.3), but the fact alone that the governing equations are Hamiltonian seems to be important for further discussion.

In addition to the integral of energy (2.2), the equations of motion (2.1) admit three more integrals due to the translational and rotational symmetry [6]:

$$Q = av_2 - \lambda x_c + \sum_{j=1}^2 \lambda_j (\tilde{x}_j - x_j), \quad P = av_1 + \lambda y_c - \sum_{j=1}^2 \lambda_j (\tilde{y}_j - y_j), \quad (2.4)$$

$$I = a(v_1 y_c - v_2 x_c) - \frac{1}{2} \lambda r_c^2 - \frac{1}{2} \sum_{j=1}^2 \lambda_j r_j^2 + \frac{1}{2} \sum_{j=1}^2 \lambda_j \left( \frac{R^2}{r_j^2} - 1 \right) (r_j, r_c). \quad (2.5)$$

The integrals  $Q$  and  $P$  are a generalization of classical linear momentum. They can also be considered as *the center of vorticity* of the vortices and the cylinder [21, 23]. For  $\lambda \neq 0$  one can choose a coordinate system in such a way that  $Q = P = 0$ , thus shifting the center of vorticity to the origin.

The Poisson brackets of the integrals  $Q$ ,  $P$  and  $I$  differ from the Lie–Poisson bracket that corresponds to the algebra  $e(2)$  by a constant (co-cycle [1]), that is,

$$\{Q, P\} = \lambda, \quad \{I, Q\} = P, \quad \{I, P\} = -Q.$$

Thus, the order of the Hamiltonian system (2.1) can be reduced by two degrees of freedom. Moreover, if

$$\lambda = 0, \quad P = Q = 0, \quad (2.6)$$

the order can be reduced by three degrees of freedom. Thus, the system of a circular cylinder and a single vortex is integrable in the sense of Liouville, and so is the system of a cylinder and two vortices if (2.6) is fulfilled.

### 2.3. Reduction by Two Degrees of Freedom

On a common level set  $P = \text{const}$ ,  $Q = \text{const}$  (in our case  $P = Q = 0$ ) the system's order can be reduced by two degrees of freedom. To do so we can solve Eqs. (2.4) for the velocities  $\mathbf{v}$ :

$$v_2 = -\frac{1}{a} \sum_{j=1}^2 \lambda_j (\tilde{x}_j - x_j), \quad v_1 = \frac{1}{a} \sum_{j=1}^2 \lambda_j (\tilde{y}_j - y_j) \quad (2.7)$$

and plug the result into (2.1). Also note that the equations governing the motion of the cylinder's center (the vector  $\mathbf{r}_c$ ) are uncoupled and can be temporarily ignored. The four equations that result (the first vector equation in the collection (2.1)) can be conveniently rewritten using complex notation (see (A.2)):

$$\dot{z}_k = \frac{dw_k(z)}{dz} = -\bar{v} + \frac{R^2 v}{z_k^2} - i\lambda_k \frac{1}{z_k - \tilde{z}_k} + i \sum_{j \neq k}^2 \lambda_j \left( \frac{1}{z_k - z_j} - \frac{1}{z_k - \tilde{z}_j} \right), \quad (2.8)$$

$$\tilde{z}_k = \frac{R^2}{\bar{z}_k} \quad k = 1, 2.$$

Here the complex variables  $z_k = x_k + iy_k$  determine the location of the vortices relative to the cylinder's center. (The cylinder's velocity should be eliminated with the help of (2.7).)

The system of equations (2.8) is Hamiltonian with the Hamiltonian function (2.2) (in which the velocities are replaced using (2.7)):

$$\begin{aligned}
 H = & \frac{1}{2a} \left( \sum_{j=1}^2 \lambda_j (\tilde{x}_j - x_j) \right)^2 + \frac{1}{2a} \left( \sum_{j=1}^2 \lambda_j (\tilde{y}_j - y_j) \right)^2 \\
 & + \frac{1}{2} \sum_{j=1}^2 \lambda_j^2 \ln(\mathbf{r}_j^2 - R^2) + \frac{1}{2} \lambda_1 \lambda_2 \ln \frac{R^4 - 2R^2(\mathbf{r}_1, \mathbf{r}_2) + \mathbf{r}_1^2 \mathbf{r}_2^2}{|\mathbf{r}_1 - \mathbf{r}_2|^2}.
 \end{aligned}
 \tag{2.9}$$

Using the Dirac reduction procedure [13], the bracket (2.3) can be reduced to the manifold  $Q = P = 0$ , thereby yielding the classical bracket obtained by Kirchhoff for the  $n$ -vortex problem:

$$\{x_i, y_i\} = \frac{1}{\lambda_i}, \quad i = 1, 2.
 \tag{2.10}$$

The equations of motion (2.8) now take the form

$$\dot{x}_i = \frac{1}{\lambda_i} \frac{\partial H}{\partial y_i}, \quad \dot{y}_i = -\frac{1}{\lambda_i} \frac{\partial H}{\partial x_i}, \quad i = 1, 2.
 \tag{2.11}$$

Thus, the cylinder can be treated as a sort of “a complicated vortex” which does not affect the Poisson bracket but seriously complicates the structure of the Hamiltonian function.

The system of equations (2.11) is invariant under rotation about the center of the cylinder and therefore admits an additional integral of motion, which coincides with the integral (2.5) (in which the velocities are replaced by the formulas (2.7)):

$$I = \sum_{j=1}^2 \lambda_j \mathbf{r}_j^2.
 \tag{2.12}$$

So the Hamiltonian system with two degrees of freedom (2.11) is integrable in the sense of Liouville.

### 3. EXPLICIT REDUCTION TO A ONE-DEGREE-OF-FREEDOM SYSTEM

Let us reduce the order of the system of equations (2.11) by one degree of freedom. Note that the bracket (2.10) is not a canonical one and the system does not seem to have any cyclic variables (the integral of motion (2.12) can hardly be treated as a *cyclic momentum*). For this reason classical methods of reduction (such as Routh’s procedure) do not straightforwardly apply here. To proceed we first switch to some relative variables which, in essence, constitutes the desired reduction (or at least its algebraic counterpart).

As new (relative) variables it is customary to choose invariants of the vector field  $\mathbf{v}_I = \{I, \cdot\}$  generated by the integral (2.12), that is,

$$p_1 = x_1^2 + y_1^2, \quad p_2 = x_2^2 + y_2^2, \quad p_3 = x_1 x_2 + y_1 y_2, \quad p_4 = x_1 y_2 - y_1 x_2.
 \tag{3.1}$$

The nonzero brackets of these variables are

$$\begin{aligned}
 \{p_1, p_3\} = \frac{2p_4}{\lambda_1}, \quad \{p_1, p_4\} = -\frac{2p_3}{\lambda_1}, \quad \{p_2, p_3\} = -\frac{2p_4}{\lambda_2}, \\
 \{p_2, p_4\} = \frac{2p_3}{\lambda_2}, \quad \{p_3, p_4\} = \frac{p_1}{\lambda_2} - \frac{p_2}{\lambda_1}.
 \end{aligned}
 \tag{3.2}$$

In terms of the new variables (3.1) the conserved quantities (2.9) and (2.12) take the form

$$H = \frac{1}{2a} \left( \sum_{j=1}^2 \frac{\lambda_j^2 (R^2 - p_j)^2}{p_j} + \frac{\lambda_1 \lambda_2 (R^2 - p_1)(R^2 - p_2)p_3}{p_1 p_2} \right)
 \tag{3.3}$$

$$\begin{aligned}
& + \sum_{j=1}^2 \frac{\lambda_j^2}{2} \ln(p_j - R^2) + \frac{\lambda_1 \lambda_2}{2} \ln \frac{R^4 - 2R^2 p_3 + p_1 p_2}{p_1 + p_2 - 2p_3} \\
& I = \lambda_1 p_1 + \lambda_2 p_2.
\end{aligned} \tag{3.4}$$

The time evolution of the variables  $p_i$  is given by  $\dot{p}_i = \{p_i, H\}$ , which in expanded notation looks like

$$\begin{aligned}
\dot{p}_1 &= \frac{2p_4}{\lambda_1} \frac{\partial H}{\partial p_3} = 2\lambda_2 p_4 (R^2 - p_1)(R^2 - p_2) \left( \frac{1}{ap_1 p_2} + \frac{1}{(p_1 + p_2 - 2p_3)(R^4 - 2R^2 p_3 + p_1 p_2)} \right), \\
\dot{p}_2 &= -\frac{2p_4}{\lambda_2} \frac{\partial H}{\partial p_3}, \quad \dot{p}_3 = -2p_4 \left( \frac{1}{\lambda_1} \frac{\partial H}{\partial p_1} - \frac{1}{\lambda_2} \frac{\partial H}{\partial p_2} \right), \\
\dot{p}_4 &= 2p_3 \left( \frac{1}{\lambda_1} \frac{\partial H}{\partial p_1} - \frac{1}{\lambda_2} \frac{\partial H}{\partial p_2} \right) + \left( -\frac{p_1}{\lambda_2} + \frac{p_2}{\lambda_1} \right) \frac{\partial H}{\partial p_3}.
\end{aligned} \tag{3.5}$$

The Poisson structure (3.2) is degenerate and its rank equals two. It is straightforward to show that the integral (3.4) and the function

$$I_1 = p_3^2 + p_4^2 - p_1 p_2 \tag{3.6}$$

are Casimir functions of the structure (3.2). (For real motions  $I_1 = 0$ .) Thus, this Hamiltonian system has exactly one degree of freedom. Next we follow the ideas of the work [3] to finally obtain this one-degree-of-freedom system in the canonical form.

In the four-dimensional space of the variables  $p_i$  the two-dimensional common level surface

$$I_1 = 0, \quad I = c \tag{3.7}$$

is the phase space of the reduced system. The structure of the symplectic leaf (3.7) is determined by the values of the strengths  $\lambda_1, \lambda_2$  [3] and by the type of the Lie algebra that corresponds to the bracket (3.2).

There are two possibilities:

1.  $\lambda_1 \lambda_2 > 0$ . Instead of  $p_1, p_2, p_3, p_4$  we choose new basis functions  $I, e_1, e_2, e_3$  given by

$$e_1 = \frac{\lambda_1 p_1 - \lambda_2 p_2}{4}, \quad e_2 = \frac{\sqrt{\lambda_1 \lambda_2}}{2} p_3, \quad e_3 = \frac{\sqrt{\lambda_1 \lambda_2}}{2} p_4. \tag{3.8}$$

The nonzero brackets read

$$\{e_1, e_2\} = e_3, \quad \{e_2, e_3\} = e_1, \quad \{e_3, e_1\} = e_2. \tag{3.9}$$

Note that this is exactly the way the standard generators of the algebra  $so(3)$  commute with each other. The leaves (3.7) are compact, diffeomorphic to two-dimensional spheres and are given by the equations

$$I = c, \quad e_1^2 + e_2^2 + e_3^2 = G^2 = \frac{c^2}{16}. \tag{3.10}$$

In this case it is customary to pick as canonical variables the cylindrical coordinates  $l$  and  $L$  (reminiscent of the Andoyer–Deprit variables from rigid body dynamics [5]) given by

$$e_1 = L, \quad e_2 = \sqrt{G^2 - L^2} \sin l, \quad e_3 = -\sqrt{G^2 - L^2} \cos l, \quad \{l, L\} = 1. \tag{3.11}$$

These coordinates are remarkable for two things: they are defined globally and therefore their use does not entail annoying odds and ends that have only peripheral relationship to the essence of the problem.

2.  $\lambda_1 \lambda_2 < 0$ . New basis functions  $I, e_1, e_2, e_3$  and their nonzero brackets (paralleling those from the algebra  $so(2, 1)$ ) now read

$$e_1 = \frac{\sqrt{-\lambda_1 \lambda_2}}{2} p_3, \quad e_2 = \frac{\sqrt{-\lambda_1 \lambda_2}}{2} p_4, \quad e_3 = \frac{\lambda_1 p_1 - \lambda_2 p_2}{4}, \tag{3.12}$$

$$\{e_1, e_2\} = -e_3, \quad \{e_2, e_3\} = e_1, \quad \{e_3, e_1\} = e_2. \tag{3.13}$$

In terms of these variables the equations for the leafs (3.7), which are single-sheet hyperboloids, can be written as

$$I = c, \quad e_3^2 - e_1^2 - e_2^2 = G^2 = \frac{c^2}{16}. \tag{3.14}$$

Canonical coordinates  $l, L$  can be introduced in the following way:

$$e_1 = \sqrt{L^2 - G^2} \cos l, \quad e_2 = \sqrt{L^2 - G^2} \sin l, \quad e_3 = L, \quad \{l, L\} = 1. \tag{3.15}$$

Thus, the system is explicitly reduced to a canonical Hamiltonian system with one degree of freedom:

$$\dot{l} = \frac{\partial H}{\partial L}, \quad \dot{L} = -\frac{\partial H}{\partial l}. \tag{3.16}$$

The Hamiltonian function  $H(L, l, c)$  is given by (3.3) in which the variables  $p_1, p_2, p_3, p_4$  should be expressed in terms of  $l$  and  $L$  using (3.10) and (3.11) if  $\lambda_1 \lambda_2 > 0$  (or using (3.14) and (3.15) if  $\lambda_1 \lambda_2 < 0$ ). We have

- for  $\lambda_1 \lambda_2 > 0$

$$\begin{aligned} H(L, l, c) = & \frac{1}{a} \left( \frac{\lambda_1 (R^2 \lambda_1 - c/2 - 2L)^2}{4L + c} + \frac{\lambda_2 (R^2 \lambda_2 - c/2 + 2L)^2}{4L - c} \right) \tag{3.17} \\ & + \frac{(2R^2 \lambda_1 - c - 4L)(2R^2 \lambda_2 - c + 4L) \sqrt{\lambda_2 \lambda_1} \sin l}{2a \sqrt{c^2 - 16L^2}} \\ & + \frac{\lambda_1^2}{2} \ln(-2R^2 \lambda_1 + c + 4L) + \frac{\lambda_2^2}{2} \ln(c - 4L - 2R^2 \lambda_2) \\ & + \frac{\lambda_1 \lambda_2}{2} \ln \left( \frac{4R^4 \lambda_1 \lambda_2 - 4R^2 \sqrt{\lambda_2 \lambda_1} \sqrt{c^2 - 16L^2} \sin l - 16L^2 + c^2}{2(c + 4L) \lambda_2 + 2\lambda_1(c - 4L) - 4\sqrt{\lambda_2 \lambda_1} \sqrt{c^2 - 16L^2} \sin l} \right) \end{aligned}$$

- for  $\lambda_1 \lambda_2 < 0$

the Hamiltonian  $H(L, l, c)$  coincides with (3.17) in which one should replace  $\sqrt{\lambda_2 \lambda_1}$  with  $\sqrt{-\lambda_2 \lambda_1}$ ,  $\sin l$  with  $\cos l$  and  $\sqrt{c^2 - 16L^2}$  with  $\sqrt{16L^2 - c^2}$ . (3.18)

#### 4. QUADRATURES FOR ABSOLUTE MOTION

Let  $\alpha$  be the angle between the radius-vector from the cylinder's center to the first vortex and the  $x$  axis; then the attitude dynamics of the vortices and the absolute motion of the cylinder are given by the relations

$$z_1 = x_1 + iy_1 = \sqrt{p_1} e^{i\alpha}, \quad z_2 = x_2 + iy_2 = \frac{p_3 + ip_4}{\sqrt{p_1}} e^{i\alpha}, \tag{4.1}$$

$$\dot{z}_c = \dot{x}_c + i\dot{y}_c = v_1 + iv_2 = -\frac{i}{a} (\lambda_1(\tilde{z}_1 - z_1) + \lambda_2(\tilde{z}_2 - z_2)). \tag{4.2}$$



Therefore, to be able to reconstruct the dynamics of the whole system from the knowledge of the relative variables  $p_i(t)$ , one needs (in addition to Eqs. (3.1)) one more equation, say, the one describing the time evolution of  $\alpha$ . From the obvious relation  $(\ln z_1)' = \frac{\dot{p}_1}{2p_1} + i\dot{\alpha}$  it follows that

$$\dot{\alpha} = \frac{\dot{y}_1 \cos \alpha - \dot{x}_1 \sin \alpha}{p_1} = -\frac{x_1 \frac{\partial H}{\partial x_1} + y_1 \frac{\partial H}{\partial y_1}}{\lambda_1 p_1}.$$

Then, by virtue of (2.8), (3.1) and (3.5), we obtain

$$\begin{aligned} \dot{\alpha} &= -\frac{1}{\lambda_1} \left( 2 \frac{\partial H}{\partial p_1} + \frac{p_3}{p_1} \frac{\partial H}{\partial p_3} \right) \\ &= \frac{R^2 + p_1}{ap_1^2} \left( \lambda_1 (R^2 - p_1) + \frac{\lambda_2 (R^2 - p_2) p_3}{p_2} \right) + \frac{\lambda_1}{R^2 - p_1} + \frac{\lambda_2 (R^2 - p_2) (R^2 (p_1 - p_3) - p_1 (p_3 - p_2))}{p_1 (p_1 + p_2 - 2p_3) (R^4 - 2R^2 p_3 + p_1 p_2)}. \end{aligned} \quad (4.3)$$

From these formulas the following statement can be obtained.

**Theorem.**

- 1) For any periodic solution to the system of equations (3.5) there exists a uniformly rotating coordinate frame whose origin moves rectilinearly such that with respect to this frame the vortices and the cylinder move along closed curves.
- 2) To equilibrium solutions  $p_i = \text{const}$ ,  $i \in \overline{1, 4}$  of (3.5) there corresponds a synchronous motion of the vortices (relative to the fixed coordinate system as well as relative to the cylinder's center) and the cylinder in concentric circles at constant speed.

*Proof.* Suppose  $p_i(t)$ ,  $i \in \overline{1, 4}$  are periodic functions with period  $T$ . From (4.3) it follows that  $\alpha(t) = \Omega t + g(t)$ , where  $g(t) = g(t + T)$  is a  $T$ -periodic function of time,  $\Omega$  is the average value of the periodic function  $\dot{\alpha}$ . Using (4.1), the coordinates of the vortices can be represented in the form

$$z_j = G_j(t) e^{i\Omega t}, \quad j = 1, 2. \quad (4.4)$$

Here  $G_1$  and  $G_2$  are  $T$ -periodic functions of time. To determine the motion of the cylinder's center, substitute (4.4) into (4.2). Integrating yields  $x_c + iy_c = At + e^{i\Omega t} G_c(t)$ . Here again  $G_c(t)$  is a  $T$ -periodic function of time; the constant  $A$  is different from zero provided that for some  $n \in \mathbb{Z}$  the resonance relation  $2\pi n = \Omega T$  holds. So in the coordinate system that moves with linear velocity  $A$  and rotates with angular velocity  $\Omega$  the paths of the vortices and the cylinder are closed. The second statement of the theorem immediately follows from (4.1), (4.2) and (4.3).  $\square$

**Remark.** For periodic solutions of the system (3.5) the resonance relation  $2\pi n = \Omega T$  is quite a rare occurrence limited to some measure zero sets (which is of interest in its own right and worthy of further study). So the trajectories of the vortices and the cylinder are almost always bounded (except for the case  $\lambda_1 = -\lambda_2$ ).

## 5. STATIONARY CONFIGURATIONS

Stationary configurations, which are partial solutions of the equations of motion, are traditionally classified into: a) static equilibrium configurations: the velocities of the vortices  $\mathbf{V}_1$ ,  $\mathbf{V}_2$  and the cylinder  $\mathbf{V}_c$  vanish, b) rigidly translating configurations  $\mathbf{V}_1 = \mathbf{V}_2 = \mathbf{V}_c = \mathbf{V} \neq 0$ ,  $\mathbf{V} = \text{const}$ , and c) relative equilibria (rigidly rotating configurations): the vortices and the cylinder uniformly rotate about a certain point.

There is quite a plethora of relative equilibria (Section 6), but there are no rigidly translating configurations or static equilibria. Unfortunately, the dynamical analog [31] of the Föppl equilibrium [14] lies beyond the current study because the linear momentum that corresponds to this equilibrium is different from zero, namely,  $P^2 + Q^2 \neq 0$ . The following proposition holds.

**Proposition.** *In this system there are no static equilibria or rigidly translating configurations.*



*Proof.* For a stationary configuration (of any type) to exist, the relative variables  $p_i$  must obviously be constant. In its turn, this can be the case provided that  $p_4 = 0$  (for example, from the first equation of the system (3.5) it follows that  $\dot{p}_1 = 0$  iff  $p_4 = 0$  because the rightmost bracketed expression is always positive). For this reason in equilibrium the vortices and the center of the cylinder lie on the same straight line. The velocity of the cylinder  $v_0$ , according to (4.2), is orthogonal to this line. Suppose that this line is momentarily aligned with the abscissa axis; then the coordinates of the vortices are  $(x_1, 0)$  and  $(x_2, 0)$ . In a rigidly translating configuration the vortices must have the same velocity  $v_0$ . By virtue of (2.8) we therefore obtain

$$\frac{v_0 R^2}{x_1^2} + \frac{\lambda_1}{x_1 - \frac{R^2}{x_1}} - \frac{\lambda_2}{x_1 - x_2} + \frac{\lambda_2}{x_1 - \frac{R^2}{x_2}} = -v_0, \quad \frac{v_0 R^2}{x_2^2} - \frac{\lambda_1}{x_2 - x_1} + \frac{\lambda_1}{x_2 - \frac{R^2}{x_1}} + \frac{\lambda_2}{x_2 - \frac{R^2}{x_2}} = -v_0. \tag{5.1}$$

Since the coordinates of the vortices and the cylinder’s velocity satisfy Eq. (4.2), we have

$$v_0 = -\frac{1}{a} \left( \lambda_1 \left( \frac{R^2}{x_1} - x_1 \right) + \lambda_2 \left( \frac{R^2}{x_2} - x_2 \right) \right).$$

Substituting this expression into (5.1), provides a homogeneous system of linear algebraic equations in the unknowns  $\lambda_1$  and  $\lambda_2$ . The determinant  $\Delta$  of the matrix of the coefficients reads

$$\Delta = A(x_1, x_2)a + B(x_1, x_2). \tag{5.2}$$

Here  $A(x_1, x_2)$  and  $B(x_1, x_2)$  are rational functions whose values (for the same  $x_1$  and  $x_2$ ) are of the same sign (see Appendix B). Since  $a > 0$ , the determinant  $\Delta \neq 0$  and the system of equations (5.1) has no other solution but  $\lambda_1 = \lambda_2 = 0$ , which proves the statement.  $\square$

## 6. PHASE PORTRAITS AND BIFURCATION ANALYSIS

All solutions to the system (3.16), which form the phase portrait, are level curves of the Hamiltonian function (3.17) or (3.18). The topology of the curves strongly depends on the value of the first integral  $I = c$ . For each fixed  $c$  the phase portrait is determined by the stationary points and singularities of the functions (3.17), (3.18). Here the term *singularity* refers to points in the vicinity of which the Hamiltonian function grows infinitely (in magnitude), meaning that one or both vortices tend to move infinitely fast along the cylinder’s boundary. Stationary points represent the solutions in which the vortices and the cylinder uniformly rotate in concentric circles.

Depending on the value of  $c$ , the system may have from zero to three stationary (fixed) points. At each point one can also evaluate the value of  $H$ , thereby getting a pair  $(c, H)$ . In the plane of the variables  $H$  and  $c$  these pairs form what is called a *bifurcation diagram*. At the points of a diagram the integrals of motion  $H$  and  $I$  of the original system (2.11) become functionally dependent. Figures 2, 4, 5, 7 show bifurcation diagrams, phase portraits of the system (3.16) and the trajectories of the vortices and the cylinder for various values of the parameters. For each domain in the diagram the number and the type of the corresponding invariant surfaces are indicated. In the figures the cylinder always starts its motion from the origin of coordinates; its final location (if it does not make a figure too messy) is also depicted.

The structure of the bifurcation diagram is determined by the sign of the product of the vortex strengths. So the cases of  $\lambda_1 \lambda_2 > 0$  and  $\lambda_1 \lambda_2 < 0$  will be considered below.

### 6.1. The Case of $\lambda_1 \lambda_2 > 0$

Without loss of generality, assume that  $0 < \lambda_1 \leq \lambda_2$ . The value of the integral  $I$  is governed by the inequality  $I = c > (\lambda_1 + \lambda_2)R^2$ . As  $c$  approaches its lower bound, the energy  $H$  goes to infinity, which now means that both vortices approach the cylinder’s boundary (Fig. 2 ( $A_1$ )). (For large values of  $c$  along the bifurcation curves  $H(c) \sim \ln c$ ; this indicates the absence of horizontal asymptotes and nonlocal bifurcations.)

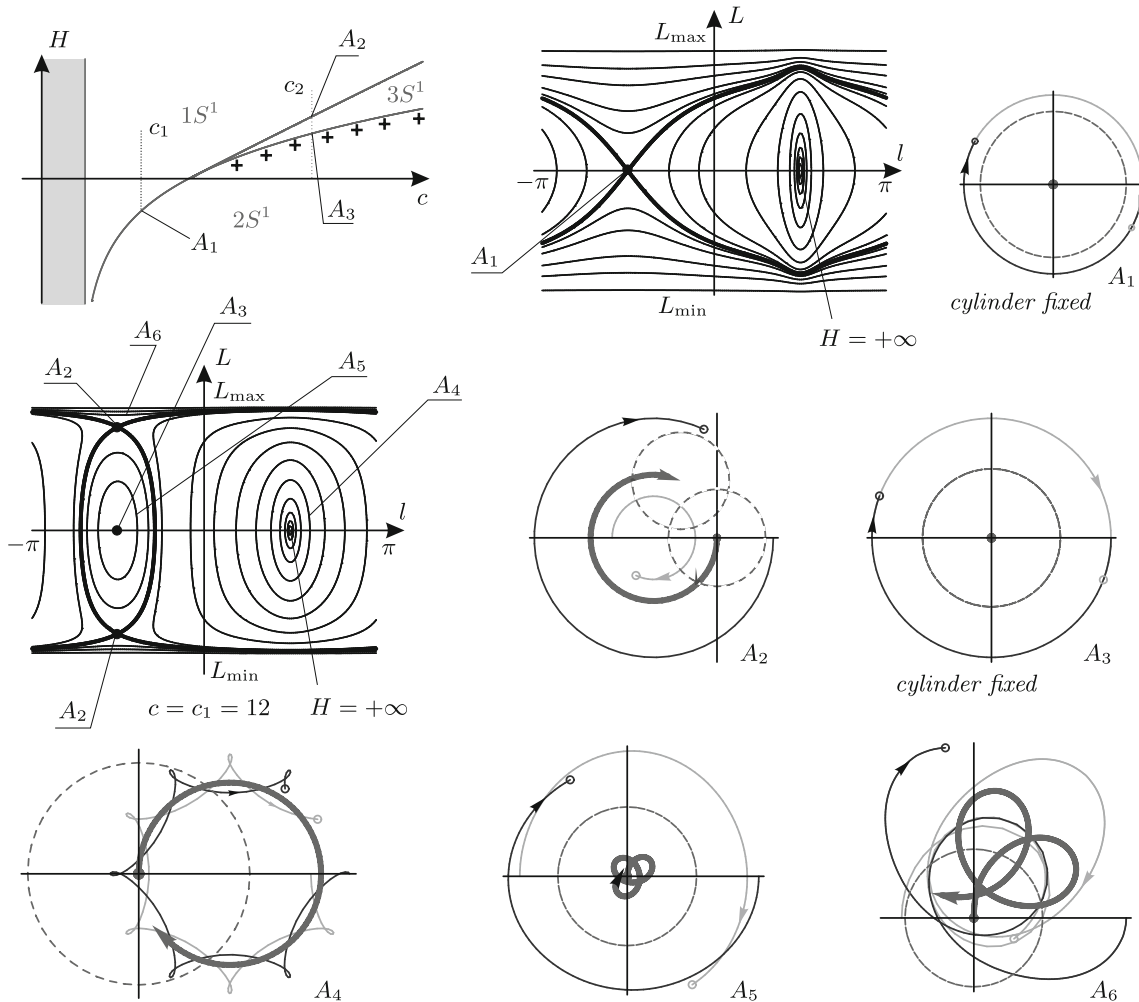


**Fig. 2.** The bifurcation diagram and the phase portraits of the system (3.17) when  $\lambda_1 = \lambda_2 = 2$ , ( $a = 1, R = 1$ ). For some phase trajectories the corresponding absolute motion of the vortices and cylinder is depicted. The path of the cylinder's center is shown as a thick line and its boundary as a dashed line, the path of the first vortex  $\lambda_1$  is a dark thin line and the path of the second vortex  $\lambda_2$  is a light thin line.

For a fixed value of  $c$  the coordinate  $L$  satisfies the inequality

$$\frac{\lambda_1 R^2}{2} - \frac{c}{4} = L_{\min} < L < L_{\max} = -\frac{\lambda_2 R^2}{2} + \frac{c}{4}. \tag{6.1}$$

In the phase portraits almost horizontal curves (close to either of the boundaries  $L_{\min}$  or  $L_{\max}$ ) represent the motion in which only one vortex is close to the cylinder (Fig. 2 ( $A_6$ )). For small values of  $I$  the structure of the phase portrait is determined by the single unstable equilibrium point  $l = -\pi/2, L = 0$  and singularity at  $l = \pi/2, L = 0$  (Fig. 2 ( $c = c_1 = 12$ )). The singularity corresponds to the motion of the vortices along the boundary of the cylinder (Fig. 2 ( $A_4$ )) and to the equilibrium point there corresponds the motion of the vortices in the same circle around the center of the cylinder, which is fixed (Fig. 2 ( $A_1$ )). As the value  $c$  of the integral  $I$  increases, so does the radius of this circle; as  $c$  exceeds a certain critical value (fork bifurcation), this solution becomes stable (Fig. 2 ( $A_3$ )), which is accompanied with the occurrence of two new unstable points. In the figure these points are identically denoted by  $A_2$  (the function  $H$  is even in  $L$ , therefore to the equilibria  $A_2$  there corresponds the same (up to axial symmetry) motion of the system).

In the case of different strengths  $\lambda_1 = 2, \lambda_2 = 3$  the lower part of the diagram detaches from the upper curve, splitting into two parts (Fig. 4). To make this bifurcation more graphic, we show how the  $L$  coordinate of the equilibria evolve as the strength  $\lambda_2$  varies from 2 to 3 (Fig. 3) (in

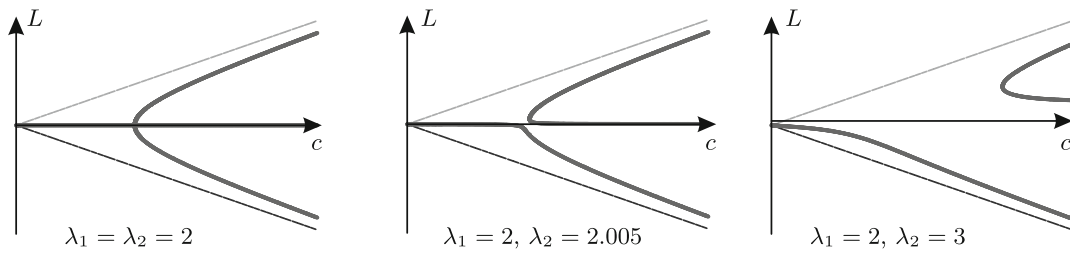


**Fig. 3.** Relative equilibria in the plane  $(c, L)$  for various values of the strength  $\lambda_2$ . The lines  $L_{\min}(c)$ ,  $L_{\max}(c)$  from (6.1) are shown in dashes.

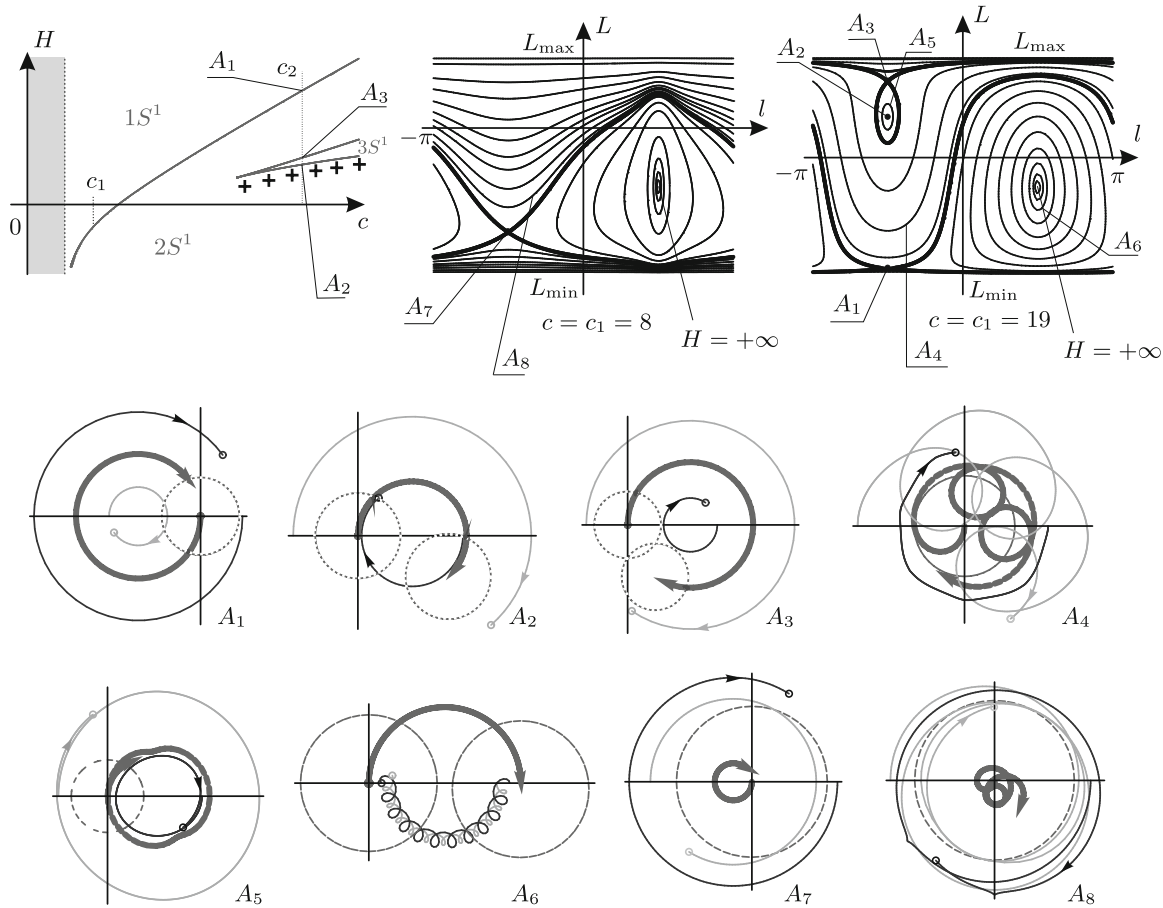


**Fig. 4.** The bifurcation diagram and the phase portraits of the system (3.17) when  $\lambda_1 = 2$ ,  $\lambda_2 = 3$  ( $a = 1$ ,  $R = 1$ ). For some phase trajectories the corresponding absolute motion of the vortices and the cylinder is depicted. The path of the cylinder's center is shown as a thick line and its boundary as a dashed line, the path of the first vortex  $\lambda_1$  is a dark thin line and the path of the second vortex  $\lambda_2$  is a thin light line.

equilibrium  $l = -\pi/2$ , meaning that the center of the cylinder and the vortices belong to the same straight line and the center is located between the vortices).

6.2. The Case of  $\lambda_1 \lambda_2 > 0$

Assume that  $0 < \lambda_1 \leq -\lambda_2$ . The trajectories of the system (3.18) lie in the region

$$L > \max(\lambda_1 R^2/2 - c/4, -\lambda_2 R^2/2 + c/4) = L_{\min}(c). \tag{6.2}$$

First, let the strengths be equal in magnitude, that is,  $\lambda_1 = -\lambda_2 = 2$ . In the bifurcation diagram (Fig. 5) there are two curves that correspond to the unstable equilibria of the system (3.18). As

mentioned above, to such equilibria there corresponds the motion of the cylinder and the vortices in concentric circles (Figs. 5(A<sub>1</sub>)–5(A<sub>3</sub>)). As  $c$  decreases, the radii of the circles along which the cylinder and the second vortex are moving get smaller, while the circle containing the first vortex expands (in Fig. 5(A<sub>2</sub>) the cylinder’s center and the first vortex move in the same circle).

As  $c$  approaches zero, the cylinder becomes practically fixed and the vortices move with almost infinite velocities in the vicinity of its boundary (Fig. 5(A<sub>3</sub>)). (For negative values of  $c$  the vortices interchange their positions and rotate in the opposite direction.)

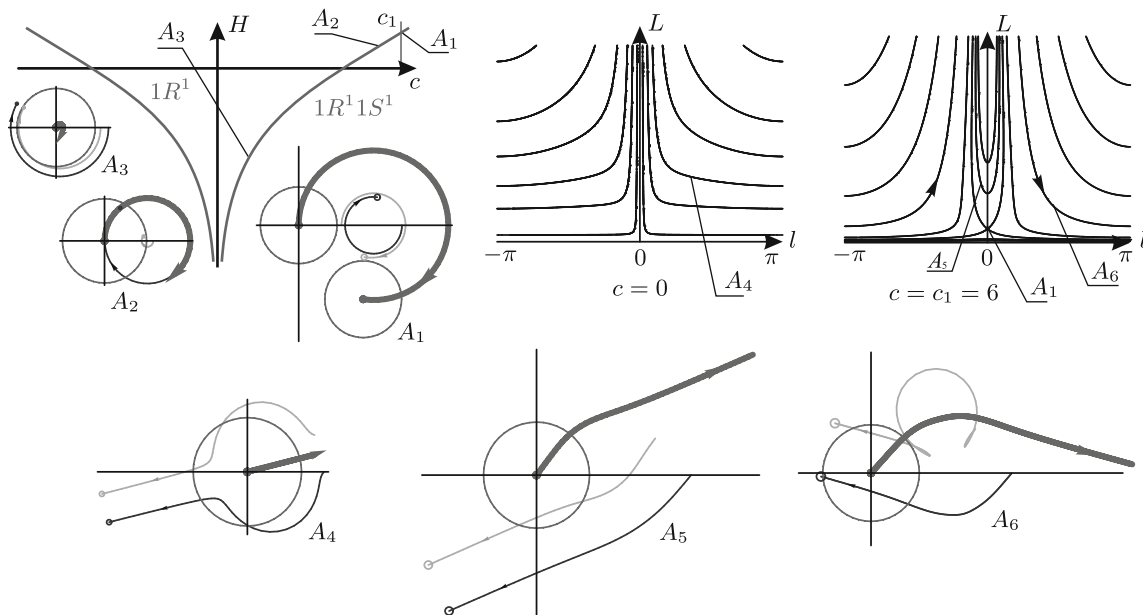


**Fig. 5.** The bifurcation diagram and the phase portraits of the system (3.17) when  $\lambda_1 = -\lambda_2 = 2$  ( $a = 1, R = 1$ ). For some phase trajectories the corresponding absolute motion of the vortices and the cylinder is depicted. The path of the cylinder’s center is shown as a thick line, the path of the first vortex  $\lambda_1$  is a dark thin line and the path of the second vortex  $\lambda_2$  is a thin light line.

Indeed, for small values of  $c$  (see (2.12)) the distances from the vortices to the center of the cylinder are practically the same (this corresponds to large negative values of the Hamiltonian  $H$ ).

In the special case  $c = 0$  there are no equilibria in the phase portraits (Fig. 5( $c = 0$ )). On every phase curve  $L \rightarrow +\infty$ ; therefore (in the limit) the vortices move as a vortex pair, while the cylinder moves almost uniformly in the opposite direction (Fig. 5(A<sub>4</sub>)). Moreover, by virtue of (2.12), the equality  $p_1 = p_2$  holds, meaning that the vortices are equally remote from the cylinder’s center. The flow is obviously symmetric about the middle perpendicular (through the center) to the segment with endpoints at the vortices. In the course of motion the center of the cylinder always belongs to this perpendicular (Fig. 5(A<sub>4</sub>)). For  $c \neq 0$  all solutions (except for equilibria and separatrices) go to infinity. Consider, for example, solution A<sub>6</sub> in Fig. 5: at the beginning the distance from the cylinder’s center to the vortices diminishes, but later it starts growing infinitely.

In the bifurcation diagram (Fig. 7) when the strengths differ in magnitude, that is,  $\lambda_1 \neq -\lambda_2$  ( $\lambda_1 = 2, \lambda_2 = -3$ ), as compared to the case  $\lambda_1 = -\lambda_2$ , the right branch fractures, while the vertical asymptote and the left branch move to the point  $c = c^* = R^2(\lambda_1 + \lambda_2)$  (for  $c = c^*$  the two arguments of the max function in (6.2) become equal). The rearrangement of the equilibrium position in the plane ( $c, L$ ) is shown in Fig. 6.

In conclusion, consider the difference between motions corresponding to “rotational” and “oscillatory” domains in phase portraits (these are, for example, the curves A<sub>6</sub> and A<sub>5</sub> in Fig. 7). According to (3.1), (3.12) and (3.15) the coordinate  $l$  determines the sign of the scalar product of the radius-vectors to the vortices from the center of the cylinder. Within the oscillatory region (curve A<sub>6</sub>) the coordinate  $l$  varies periodically within certain limits, while in the rotational domain

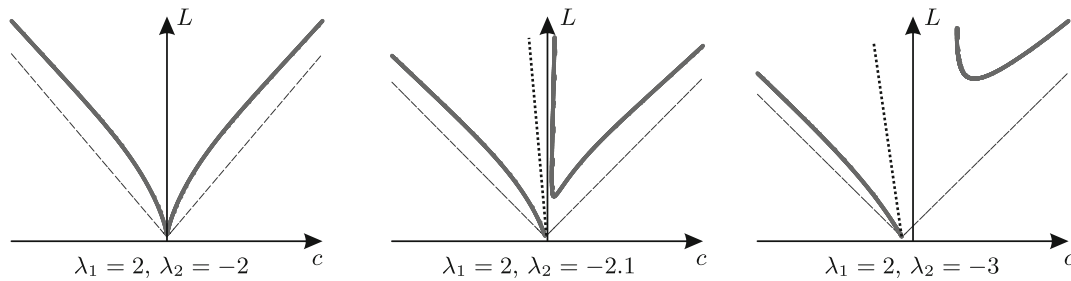


**Fig. 6.** Relative equilibria in the plane  $(c, L)$  for various values of the strength  $\lambda_2$ . The line  $L_{\min}(c)$  (see (6.2)) is shown in dashes. The dash-dotted line represents the locus of singularities of the Hamiltonian (3.18).

(curve  $A_5$ ) it grows linearly. Thus, in the oscillatory region the vortices move in a somewhat synchronous manner, executing approximately the same number of turns about the center of the cylinder in equal spans of time, while in the rotational region the angular distance between the vortices grows infinitely. For example, in Fig. 7 ( $A_5$ ) the first vortex has evidently performed less turns around the cylinder as compared to the second vortex (see also Figs. 4 ( $A_2$ ), 4 ( $A_4$ )).

### 7. CONCLUSION

Analytical and numerical evidence has shown that 1) if  $\lambda_1 \neq -\lambda_2$ , all solutions (except perhaps for a set of initial data of zero measure) of Eqs. (3.5) are periodic; the corresponding motion of the vortices and cylinder (w.r.t. the fixed coordinate frame) is bounded, 2) for  $\lambda_1 = -\lambda_2$  almost all solutions to (3.5) are not bounded, and the cylinder+vortices system travels to infinity; in so doing the vortices (at least in the limit) move nearly uniformly in parallel straight lines, while the cylinder moves also in a straight line in a nearly opposite direction. Thus, the relative motion of the vortices proves to be unbounded: the distance between them and the cylinder grows infinitely (see, for example, Figs. 5 ( $A_4$ )–5 ( $A_6$ )).

The following hypothesis seems plausible: *the absolute motion of the cylinder is bounded if and only if so is the relative motion of the vortices.*

### APPENDIX A

A body in a perfect fluid is subject to the following hydrodynamic reactions.

1) the moment and the force caused by the added mass effect [20] (in the case of a circular cylinder, one can imagine that there is no fluid while the cylinder’s mass is augmented by the mass of the fluid it displaces); given that there are no tangential forces, the net moment of forces acting on the cylinder is zero.

2) Joukowski lift [20], which reads

$$-\varrho\Gamma\mathbf{v} \times \mathbf{e}_3,$$

where  $\varrho$  is the fluid density,  $\mathbf{v}$  is the body velocity,  $\Gamma$  is the circulation, and the unit vector  $\mathbf{e}_3$  is orthogonal to the plane of the motion.

3) the force caused by a vortex of strength  $\Gamma_j$  is [26]:

$$i\varrho\Gamma_j \left( \dot{\mathbf{r}}_j - \dot{\tilde{\mathbf{r}}}_j \right).$$

This force is orthogonal to the difference of the velocities of two points: 1) of the point at which the vortex is currently located and 2) of its inverse image about the cylinder’s boundary (Fig. 1).

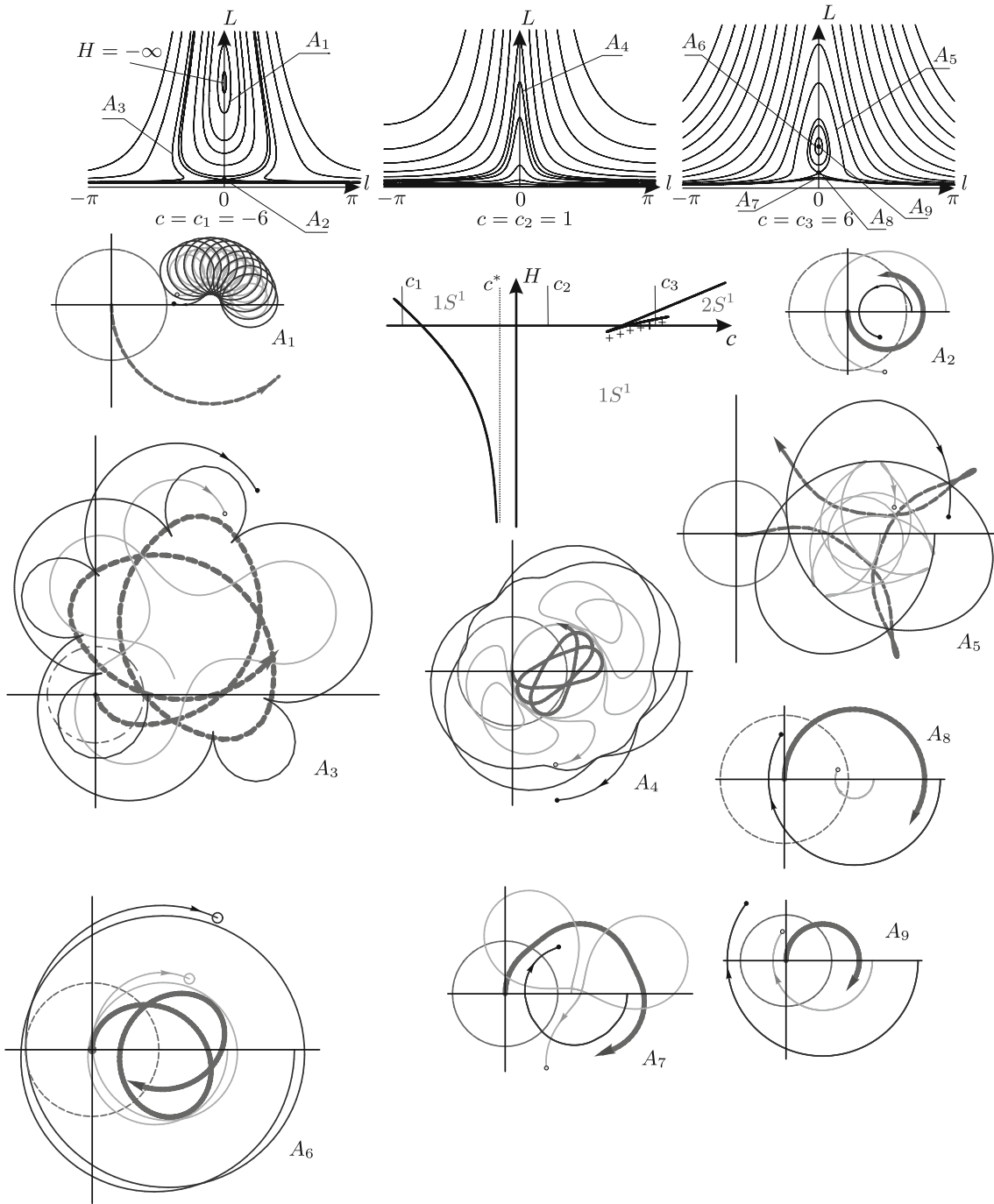


**Fig. 7.** The bifurcation diagram and the phase portraits of the system (3.17) when  $\lambda_1 = 2, \lambda_2 = -3, a = 1, R = 1$ . For some phase trajectories the corresponding absolute motion of the vortices and cylinder is depicted. The path of the cylinder's center is shown as a thick line, the cylinder itself is shown in dashes, the path of the first vortex  $\lambda_1$  is a dark thin line and the path of the second vortex  $\lambda_2$  is a thin light line.

In the domain exterior to the cylinder the complex velocity potential reads

$$w(z) = -\frac{(v_1 + iv_2)R^2}{z} - i\lambda_1 \ln(z - z_1) + i\lambda_1 \ln(z - \tilde{z}_1) - i\lambda_2 \ln(z - z_2) + i\lambda_2 \ln(z - \tilde{z}_2). \quad (\text{A.1})$$

Here  $v_1 + iv_2$  is the complex velocity of the center of the cylinder,  $z_k = x_k + iy_k, k = 1, 2$  are the positions of the vortices relative to the center of the cylinder. At the inverse image points  $\tilde{z}_k = \frac{R^2}{\bar{z}_k}$

there are vortices with opposite strengths, thereby providing the impermeable condition on the boundary.

Denote by  $\varphi_k(\mathbf{r})$  the real part of the potential (A.1) with no singularity at the position of the  $k$ -th vortex. For example,

$$\begin{aligned} \varphi_1(\mathbf{r}) &= \operatorname{Re}(w_1(z)), \\ w_1(z) &= -\frac{(v_1 + iv_2)R^2}{z} - i\lambda_2 \ln(z - z_2) + i\lambda_2 \ln(z - \tilde{z}_2) + i\lambda_1 \ln(z - \tilde{z}_1). \end{aligned} \tag{A.2}$$

### APPENDIX B

The rational functions  $A$  and  $B$  in the expression of the determinant (5.2) look like

$$A = \frac{x_1}{x_2^3} \cdot \frac{R^4 - x_2^4}{R^2 - x_1^2} + \frac{x_2}{x_1^3} \cdot \frac{R^4 - x_1^4}{R^2 - x_2^2} - \frac{(R^2 - x_1^2)(R^2 - x_2^2)}{x_1^2 x_2^2}, \tag{B.1}$$

$$B = \frac{x_1 x_2}{(R^2 - x_1^2)(R^2 - x_2^2)} + \frac{(R^2 - x_1^2)(R^2 - x_2^2)}{(x_1 - x_2)^2 (R^2 - x_1 x_2)^2}. \tag{B.2}$$

Below we show that  $A(x_1, x_2) \cdot B(x_1, x_2) > 0$  for  $|x_i| > R, i = 1, 2$ .

**1.**  $x_1 x_2 > 0$ . Obviously,  $B > 0$ . Let us prove that  $A > 0$ . The sum of the first two terms in  $A$  satisfy the inequality

$$\frac{x_1}{x_2^3} \cdot \frac{R^4 - x_2^4}{R^2 - x_1^2} + \frac{x_2}{x_1^3} \cdot \frac{R^4 - x_1^4}{R^2 - x_2^2} \geq 2\sqrt{\frac{(R^2 + x_1^2)(R^2 + x_2^2)}{x_1^2 x_2^2}}.$$

It remains to show that this lower bound is not less than the last summand in  $A$ :

$$\begin{aligned} 2\frac{\sqrt{(R^2 + x_1^2)(R^2 + x_2^2)}}{x_1 x_2} &\geq \frac{(R^2 - x_1^2)(R^2 - x_2^2)}{x_1^2 x_2^2} \Leftrightarrow \\ 4(R^2 + x_1^2)(R^2 + x_2^2) &\geq \frac{(R^2 - x_1^2)^2}{x_1^2} \frac{(R^2 - x_2^2)^2}{x_2^2}. \end{aligned}$$

The latter follows immediately from the obvious inequality  $2(R^2 + y) \geq (R^2 - y)^2/y$ , which is valid for  $y > R^2$ . Thus, for  $x_1 x_2 > 0$  both  $A$  and  $B$  are positive.

**2.**  $x_1 x_2 < 0$ . Here  $A < 0$ . Let us show that also  $B < 0$ . One can straightforwardly check that

$$0 < \frac{R^2 - x_1^2}{R^2 - x_1 x_2} \frac{R^2 - x_2^2}{R^2 - x_1 x_2} < 1.$$

Hence,

$$B < \frac{x_1 x_2}{(R^2 - x_1^2)(R^2 - x_2^2)} + \frac{1}{(x_1 - x_2)^2} = \frac{R^2 - x_1 x_2}{(R^2 - x_1^2)(R^2 - x_2^2)} \cdot (-x_1^2 - x_1 x_2 - x_2^2 + R^2).$$

The first factor is positive, while the second is negative. Therefore,  $B < 0$ .

### FUNDING

The work of S. V. Sokolov was partially supported by the Russian Science Foundation, grant nos.19-71-30012, and the Russian Foundation for Basic Research, grants no.18-29-10051-mk and 20-01-00399.

### CONFLICT OF INTEREST

The authors declare that they have no conflicts of interest.



## REFERENCES

1. Arnol'd, V. I., *Mathematical Methods of Classical Mechanics*, 2nd ed., Grad. Texts in Math., vol. 60, New York: Springer, 1997.
2. Bizyaev, I. A. and Mamaev, I. S., Dynamics of a Pair of Point Vortices and a Foil with Parametric Excitation in an Ideal Fluid, *Vestn. Udmurtsk. Univ. Mat. Mekh. Komp. Nauki*, 2020, vol. 30, no. 4, pp. 618–627 (Russian).
3. Bolsinov, A. V., Borisov, A. V., and Mamaev, I. S., Lie Algebras in Vortex Dynamics and Celestial Mechanics: 4, *Regul. Chaotic Dyn.*, 1999, vol. 4, no. 1, pp. 23–50.
4. Borisov, A. V. and Kurakin, L. G., On the Stability of a System of Two Identical Point Vortices and a Cylinder, *Proc. Steklov Inst. Math.*, 2020, vol. 310, pp. 25–31; see also: *Tr. Mat. Inst. Steklova*, 2020, vol. 310, pp. 33–39.
5. Borisov, A. V. and Mamaev, I. S., *Rigid Body Dynamics: Hamiltonian Methods, Integrability, Chaos*, Izhevsk: R&C Dynamics, Institute of Computer Science, 2005 (Russian).
6. Borisov, A. V. and Mamaev, I. S., An Integrability of the Problem on Motion of Cylinder and Vortex in the Ideal Fluid, *Regul. Chaotic Dyn.*, 2003, vol. 8, no. 2, pp. 163–166.
7. Borisov, A. V. and Mamaev, I. S., On the Motion of a Heavy Rigid Body in an Ideal Fluid with Circulation, *Chaos*, 2006, vol. 16, no. 1, 013118, 7 pp.
8. Borisov, A. V., Mamaev, I. S., and Ramodanov, S. M., Dynamics of a Circular Cylinder Interacting with Point Vortices, *Discrete Contin. Dyn. Syst. Ser. B*, 2005, vol. 5, no. 1, pp. 35–50.
9. Borisov, A. V., Mamaev, I. S., and Vetchanin, E. V., Self-Propulsion of a Smooth Body in a Viscous Fluid under Periodic Oscillations of a Rotor and Circulation, *Regul. Chaotic Dyn.*, 2018, vol. 23, nos. 7–8, pp. 850–874.
10. Borisov, A. V., Ryabov, P. E., and Sokolov, S. V., Bifurcation Analysis of a Problem on the Motion of a Cylinder and a Point Vortex in an Ideal Fluid, *Math. Notes*, 2016, vol. 99, nos. 5–6, pp. 834–839; see also: *Mat. Zametki*, 2016, vol. 99, no. 6, pp. 848–854.
11. Borisov, A. V., Vetchanin, E. V., and Mamaev, I. S., Motion of a Smooth Foil in a Fluid under the Action of External Periodic Forces: 1, *Russ. J. Math. Phys.*, 2019, vol. 26, no. 4, pp. 412–427.
12. Chaplygin, S. A., On the Action of a Plane-Parallel Air Flow upon a Cylindrical Wing Moving within It, in *The Selected Works on Wing Theory of Sergei A. Chaplygin*, San Francisco: Garbell Research Foundation, 1956, pp. 42–72.
13. Dirac, P. A. M., Generalised Hamiltonian Dynamics, *Can. J. Math.*, 1950, vol. 2, pp. 129–148.
14. Föppl, L., *Wirbelbewegung hinter einem Kreiszyylinder*, München: Verl. d. Königlich-Bayerischen Akad. d. Wiss., 1913.
15. Hartmann, D., Schneiders, L., Schröder, W., and Shashikanth, B., On the Interaction of a Vortex Pair with a Freely Moving Cylinder, in *40th Fluid Dynamics Conference and Exhibit (Chicago, Ill., 2010)*, AIAA 2010-4749, 19 pp.
16. Kadtke, J. B. and Novikov, E. A., Chaotic Capture of Vortices by a Moving Body: 1. The Single Point Vortex Case, *Chaos*, 1993, vol. 3, no. 4, pp. 543–553.
17. Kelly, S. D. and Hukkeri, R. B., Mechanics, Dynamics, and Control of a Single-Input Aquatic Vehicle With Variable Coefficient of Lift, *IEEE Trans. Robot.*, 2006, vol. 22, no. 6, pp. 1254–1264.
18. Kanso, E. and Oskouei, B. Gh., Stability of a Coupled Body-Vortex System, *J. Fluid Mech.*, 2008, vol. 600, pp. 77–94.
19. Kilin, A. A., Borisov, A. V., and Mamaev, I. S., The Dynamics of Point Vortices Inside and Outside a Circular Domain, in *Basic and Applied Problems of the Theory of Vortices*, A. V. Borisov, I. S. Mamaev, M. A. Sokolovskiy (Eds.), Izhevsk: R&C Dynamics, Institute of Computer Science, 2003, pp. 414–440 (Russian).
20. Kochin, N. E., Kibel, I. A., and Roze, N. V., *Theoretical Hydrodynamics*, New York: Wiley, 1964.
21. Kirchhoff, G., *Vorlesungen über mathematische Physik: Vol. 1. Mechanik*, Leipzig: Teubner, 1876.
22. Kozlov, V. V., On a Heavy Cylindrical Body Falling in a Fluid, *Izv. Ross. Akad. Nauk Mekh. Tverd. Tela*, 1993, no. 4, pp. 113–117 (Russian).
23. Lamb, H., *Hydrodynamics*, 6th ed., New York: Dover, 1945.
24. Mamaev, I. S. and Bizyaev, I. A., Dynamics of an Unbalanced Circular Foil and Point Vortices in an Ideal Fluid, *Phys. Fluids*, 2021, vol. 33, no. 8, 087119, 18 pp.
25. Michelin, S. and Llewellyn Smith, S. G., Falling Cards and Flapping Flags: Understanding Fluid–Solid Interactions Using an Unsteady Point Vortex Model, *Theor. Comput. Fluid Dyn.*, 2010, vol. 24, nos. 1–4, pp. 195–200.
26. Ramodanov, S. M., Motion of a Circular Cylinder and a Vortex in an Ideal Fluid, *Regul. Chaotic Dyn.*, 2001, vol. 6, no. 1, pp. 33–38.

27. Ramodanov, S. M., On the Influence of Circulation on the Behavior of a Rigid Body Falling in a Fluid, *Izv. Ross. Akad. Nauk Mekh. Tverd. Tela*, 1996, no. 5, pp. 19–24 (Russian).
28. Ramodanov, S. M., Motion of a Circular Cylinder and  $N$  Point Vortices in a Perfect Fluid, *Regul. Chaotic Dyn.*, 2002, vol. 7, no. 3, pp. 291–298.
29. Ryabov, P. E. and Sokolov, S. V., Phase Topology of Two Vortices of Identical Intensities in a Bose—Einstein Condensate, *Russian J. Nonlinear Dyn.*, 2019, vol. 15, no. 1, pp. 59–66.
30. Shashikanth, B. N., Poisson Brackets for the Dynamically Interacting System of a 2D Rigid Cylinder and  $N$  Point Vortices: The Case of Arbitrary Smooth Cylinder Shapes, *Regul. Chaotic Dyn.*, 2005, vol. 10, no. 1, pp. 1–14.
31. Shashikanth, B. N., Symmetric Pairs of Point Vortices Interacting with a Neutrally Buoyant Two-Dimensional Circular Cylinder, *Phys. Fluids*, 2006, vol. 18, no. 12, 127103, 17 pp.
32. Shashikanth, B. N., Marsden, J. E., Burdick, J. W., and Kelly, S. D., The Hamiltonian Structure of a 2D Rigid Circular Cylinder Interacting Dynamically with  $N$  Point Vortices, *Phys. Fluids*, 2002, vol. 14, pp. 1214–1227.
33. Sokolov, S. V., Falling Motion of a Circular Cylinder Interacting Dynamically with  $N$  Point Vortices, *Nelin. Dinam.*, 2014, vol. 10, no. 1, pp. 59–72 (Russian).
34. Sokolov, S. V., Falling Motion of a Circular Cylinder Interacting Dynamically with a Vortex Pair in a Perfect Fluid, *Vestn. Udmurtsk. Univ. Mat. Mekh. Komp. Nauki*, 2014, no. 2, pp. 86–99 (Russian).
35. Sokolov, S. V. and Koltsov, I. S., Scattering of the Point Vortex by a Falling Circular Cylinder, *Dokl. Phys.*, 2015, vol. 60, no. 11, pp. 511–514.
36. Sokolov, S. V. and Ramodanov, S. M., Falling Motion of a Circular Cylinder Interacting Dynamically with a Point Vortex, *Regul. Chaotic Dyn.*, 2013, vol. 18, nos. 1–2, pp. 184–193.
37. Sokolov, S. V. and Ryabov, P. E., Bifurcation Analysis of the Dynamics of Two Vortices in a Bose—Einstein Condensate. The Case of Intensities of Opposite Signs, *Regul. Chaotic Dyn.*, 2017, vol. 22, no. 8, pp. 976–995.
38. Sokolov, S. V. and Ryabov, P. E., Bifurcation Diagram of the Two Vortices in a Bose—Einstein Condensate with Intensities of the Same Signs, *Dokl. Math.*, 2018, vol. 97, no. 3, pp. 286–290; see also: *Dokl. Akad. Nauk*, 2018, vol. 480, no. 6, pp. 652–656.
39. Tallapragada, P. and Kelly, S. D., Reduced-Order Modeling of Propulsive Vortex Shedding from a Free Pitching Hydrofoil with an Internal Rotor, in *American Control Conference (Washington, DC, 2013)*, pp. 615–620.